A Two-Stage Coordination Strategy for the Control of Distributed Storage at the Household Level -Arbitrage Between Users Preferences and Distribution Grid Objectives

Rémy Rigo-Mariani, Vincent Debusschere

A Two-Stage Coordination Strategy for the Control of Distributed Storage at the Household Level – Arbitrage Between Users Preferences and Distribution Grid Objectives

Rémy Rigo-Mariani[a], Vincent Debusschere[a]

[a] *Univ. Grenoble Alpes, CNRS, Grenoble INP, G2Elab,38000 Grenoble, France*

ARTICLE INFO

Keywords:
Distributed Storage,
Coordination,
ADMM,
Day-ahead commitment,
Near real-time control,

ABSTRACT

This paper focuses on a two-stage coordination strategy for distributed storage systems located at the end-user level. A first day-ahead commitment stage lies on the Alternating Direction Method of Multipliers adapted to a decentralized problem in which the followers and leaders exchange prices (Lagrangian)/quantities information over iterations. Then a three-step coordination is proposed for real-time control to guarantee a fast convergence while trying to remain as close as possible to the profiles scheduled in the look-ahead stage. Specific attention is attached to the end-users' objective function and their willingness to respond to coordinator signals. A layout of up to 100 households is simulated with the performances assessed regarding the trade-off between loss of revenue and global objective improvements. The impacts of load and solar generation forecasts errors are also investigated along with the effect of storage parameters. Obtained results highlight the need for a trade-off between the targeted objective in the look-ahead phase, and the confidence that it can be fulfilled in real-time.

Table 1: Nomenclature of the main symbols

Sets:		**Parameters:**	
$t \in T$	set of time steps (both day-ahead or real-time)	$g^0_{n,t}$	available generation at house *n* at time *t* (kW)
$n \in N$	set of households	$\overline{s_n}, \overline{e_n}$	battery capacity at house *n* (kW, kWh)
Variables:		$\underline{soc}, \overline{soc}$	lower/upper bound for the state of charge (%)
$g_{n,t}, g^-_{n,t}$	generation and curtailment at house *n* at time *t* (kW)	soc_0	initial state of charge (%)
$s^+_{n,t}, s^-_{n,t}$	battery charge/discharge at house *n* at time *t* (kW)	η	battery efficiency (-)
$u^{s+}_{n,t}$	battery charging at house *n* at time *t* {0,1}	π^+_t, π^-_t	Purchase/sell price at time *t* (€/kWh)
$soc_{n,t}$	state of charge at house *n* at the end of timestep *t* (%)	dt	time step – day-ahead: 30 min, real-time: 5 min
$p^+_{n,t}, p^-_{n,t}$	grid import/export at house *n* at time *t* (kW)	$.^{da}$	values predicted/computed in the day-ahead phase
p_t	PCC power at time *t* (kW)	$.^{rt}$	values measured/computed in the real-time phase
$\boldsymbol{x_{n,t}}, \boldsymbol{X_t}$	local and aggregated control vectors at time *t* (-)	Δsoc	state of charge bandwidth in the real-time phase (%)

1. Introduction

While they allow reduced carbon emissions and higher self-sufficiency ratios for electricity usage, renewable energy resources challenge the management of legacy power systems due to volatile generation profiles and the difficulty of predictability/controllability. One envisioned way to cope with those shortcomings is the integration of flexibilities in the form of energy storage, demand response, and/or partially controllable distributed generation [1]. Those flexibilities means can consist of both distribution scale assets (in the MVA range) connected to the MV networks and small-scale installations at the end-user level ('behind the meter') [1]. As an example of single house energy management strategy [2] provides a comprehensive optimization-based home energy management strategy (HEMS), while considering flexible electrical appliances. Also, the work introduces a trade-off between users' preferences (e.g. minimum energy bill), and

values for grid operators (e.g. smoothened power profiles). More flexibilities and interesting tradeoff can be leverage when considering a pool of users with assets 'behind the meter'. In such cases flexibility management can be challenging due to a potentially great number of resources and the need to deal with third-party owners -i.e. privacy by design for the control schemes.

Typically, coordination schemes are proposed to uptake the benefits of the resources, ranging from fully distributed (peer-to-peer) approaches [3] to more decentralized strategies (leader-followers) [4]. In practice, an equilibrium has to be found between the individual owners' objectives (e.g., electricity bill) and the global system targets/constraints (e.g., losses, voltage, transformer loading). Decomposition techniques with the use of complementarity problems can be implemented to estimate the system equilibrium. Typically, approaches take advantage of the convexity and differentiability of the considered functions (objective and constraints) to represent the lower-level problems (e.g., end-users) by their equivalent Karsh-Kuhn-Tucker conditions [5]. If those methods allow identifying the equilibrium, they cannot be used in the operational phase to reach this equilibrium – as they ultimately rely on centralized formulations of multi-level problems. In practice, iterative processes shall be implemented with the exchange of information between the stakeholders (typically price/quantity signals). For instance, [4] proposes a decentralized strategy in which different users coordinate to minimize their bills and maximize the share of renewable at the community level while paying attention to the forecast errors. In [6], a decentralized scheme is adopted for voltage regulation in the distribution grid with successive back-and-forth communication between roots and leaves. Among the distributed optimization techniques, the Alternating Direction Method of Multipliers (ADMM) has gained interest in the field of distributed energy resource management in the past years [7]. This algorithm proceeds in iterations where the agents optimize their individual objectives while converging toward consensus (we talk here of C-ADMM). In this paper, the consensus algorithm is adapted to a decentralized strategy with one coordinator agent driving the consensus values before forwarding them to the followers. The method is implemented for a set of households that minimize their energy bill while the global objective is to smooth the overall power (e.g., minimize the delivery transformer loading and back-feed power). Attention is also paid to the pricing policy and control abilities at the house level. Especially, the paper investigates the willingness of users to respond to coordinator signals and their impact on the overall objectives.

If the previous approaches can be applied in a look-ahead phase (e.g., day-ahead scheduling) where the computational time is not a concern, real-time (or near real-time) management requires faster convergence. Similar to typical microgrid control architectures, hierarchical methodologies can be considered with a day-ahead phase followed by an online adaptation of the scheduled controller. As explained in [8] the objective of such a real-time procedure is to cope with unavoidable forecast errors, or unpredicted events (e.g., loss of equipment). One particular objective of real-time operations can be to remain as close as possible to the power profiles scheduled and committed in the look-ahead phase. This is especially of interest for power system operators with a reduced need for carbon-intensive energy reserves to fulfill the demand/load balance in real-time thanks to more predictable power profiles at the end-user level. Both [9] and [10] adopt ADMM for the real-time coordination of users paying attention to the fulfillment of distribution grid constraints (i.e., current/voltage limitation). However, the number of iterations before convergence cannot be controlled with regular ADMM implementations. Thus, this paper proposes a three-step coordination strategy to ensure convergence in real-time operation. Inspired by the recent literature (e.g., [11]) on the coordination between Transmission and Distribution System Operators (TSO-DSO), the idea is to coordinate the real-time operation of a set of users based on their declaration of 'feasible region' in terms of reachable values of active grid power at their meter level (i.e., import/export). The main contributions of the papers are:

- The implementation of a two-stage decentralized management strategy for day-ahead and near real-time operations of a pool of users with privacy by design.

- The ability to account for user preferences and a global objective from the DSO's perspective based on power profile smoothing and predictability.
- Scalability tests up to one hundred coordinated users and sensitivity analysis on systems settings, control parameters and quality of forecasts.

The rest of the paper is organized as follows. Section 2 describes the main model equations for the operation of solar and storage assets along with both household and coordinator's objectives. Section 3 presents the ADMM based coordination for the look-ahead operational scheduling of the users' assets. Section 4 describes the real-time management strategy that adapts the scheduled controls. Results are presented in Section 5 with scalability tests and sensitivity analysis before conclusions are drawn in Section 6.

2. Case Study and Generic Model

2.1. Considered System and Two-stage Management Strategy

The case study investigated in this paper consists of the decentralized control of a set of households ($n \in N$). Each house is equipped with a solar generator and an energy storage system and controls its assets over a given time horizon T ($t \in T$) with fixed time steps dt (Figure 1). The different households are controlled to fulfill an arbitrage between their objectives (inner problem) and the overall coordination targets (upper problem). This coordinator can be located at the feeder level (or point of common coupling - PCC). The proposed management consists of a two-stage strategy with *i)* the day-ahead commitment on the grid power profiles (at both the household and coordinator levels) and *ii)* a real-time adaption of the controls to fulfill the commitment as much as possible (a deviation metric will be specifically introduced further). Both stages rely on the coordination between individuals and the coordinator with the exchanges of prices/quantity/reference signals. Specific attention is attached to privacy concerns with a coordinator that cannot access user information 'behind the meter' (i.e., individual load or generation profiles and individual asset controls). Note that the distribution grid connecting houses is not considered – i.e., no load flow analysis, voltage concerns, and/or losses minimization issues. The management lies in the optimization of the active load flows only.

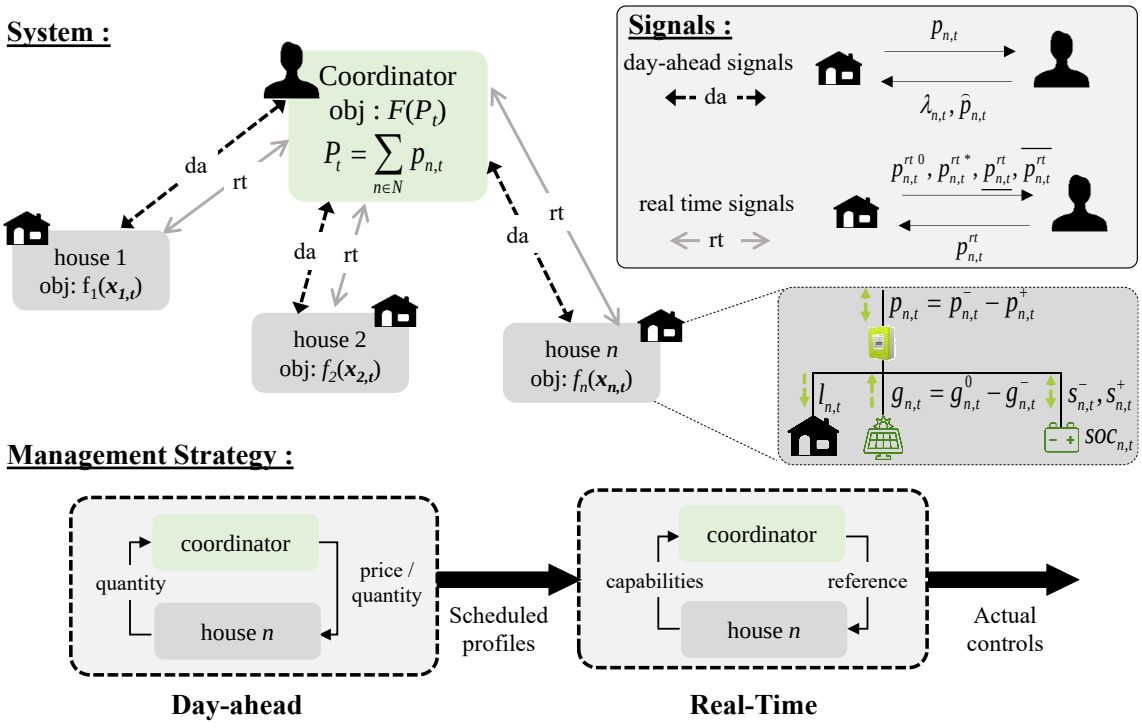

Figure 1: Considered case study and two-stage management strategy.

2.2. Generic Model Equations

The controls and state variables of each household over the time horizon are stored in a matrix $\boldsymbol{x_{n,t}}$ with the storage discharge/charge power ($s^-_{n,t}$, $s^+_{n,t}$) and energy ($e_{n,t}$), the export/import power with the main grid ($p^-_{n,t}$, $p^+_{n,t}$), computed for a given load ($l_{n,t}$) and generation profiles ($g_{n,t}$). The generation results from the available resources $g^0_{n,t}$ and the ability to curtail part or totality of the production($g^-_{n,t}$). As furtherly developed, the households' objective depends on the control phase considered (i.e., day-ahead or real-time) and on the investigated scenario for the billing mechanisms. A generic objective is denoted $f_n(\boldsymbol{x_{n,t}})$. The management problem at the house level ultimately takes the form of an optimization problem expressed in (1). Traditional linear constraints account for the power balance at each time step, (2), and the storage operating limitations (3), and energy, (4), about the maximum power $\overline{s_n}$ and capacity $\overline{e_n}$. A conventional periodicity constraint is introduced to ensure that the storage returns to its initial value at the end of the simulated period, (5) [12] with the stored energy computed with the round trip efficiency η, (6). Note that the state of charge is given at the beggining of the corresponding time step. Finally, potential curtailment of generation is represented by constraints (7) and (8). In practice, curtailment is possible with a degradation of the MPPT (maximum power point tracking) of the solar generator, which translates in a modified voltage reference at the level of the photovoltaic modules [13]. Also, Note that taking into account this storage efficiency consists of accounting for both charging and discharging losses while disaggregating two operating modes thanks to a binary variable $u^{s+}_{n,t}$ (for charging in (3)) which requires the implementation of mixed integer programming problems. For faster computational time and the simulation of longer time horizons, the storage efficiency can then be set to unity, at the cost of model simplification. A nomenclature of the main symbols used is given in Table 1.

$$\text{obj}: \min_{\boldsymbol{x_{n,t}}=\left\{s^-_{n,t},s^+_{n,t},e_{n,t},g^-_{n,t},p^-_{n,t},p^+_{n,t}\right\}} f_n\left(\boldsymbol{x_{n,t}}\right) \tag{1}$$

Subject to :

$$p^+_{n,t} + g_{n,t} + s^-_{n,t} = l_{n,t} + s^+_{n,t} + p^-_{n,t} \qquad \forall t \in T \tag{2}$$

$$0 \le s^+_{n,t} \le \overline{s_n} \times u^{s+}_{n,t} \;,\; 0 \le s^-_{n,t} \le \overline{s_n} \times \left(1 - u^{s+}_{n,t}\right) \quad \forall t \in T \tag{3}$$

$$\underline{soc} \le soc_{n,t} \le \overline{soc} \quad \forall t \in T \tag{4}$$

$$soc_{t=0} = soc_{t=T} = soc_0 \tag{5}$$

$$soc_t = soc_{n,t-1} + \left(s^+_{n,t} \times \eta - s^-_{n,t} / \eta\right) \times \frac{100 \times dt}{\overline{e_n}} \quad \forall t \in T - \{1\} \tag{6}$$

$$0 \le g^-_{n,t} \le g^0_{n,t} \quad \forall t \in T \tag{7}$$

$$g_{n,t} = g^0_{n,t} - g^-_{n,t} \quad \forall t \in T \tag{8}$$

Once all the controls in the subsystems are defined (matrices $\boldsymbol{x_{n,t}}$ aggregated in $\boldsymbol{X_t}$), it is possible to compute the objective at the coordination layer. In practice, the coordination can be performed at an energy community level, or more concretely at the point of common coupling (PCC) of the different users (i.e., MV/LV transformer). The DSO may then be in charge of the communication exchanges with the individual houses in the course of the coordination strategy. One typical objective at the delivery transformer level is the peak-to-average ratio (PAR) which targets smooth imported power profiles [14]. In this paper, and to penalize both upstream and downstream flows, the overall objective is defined as the square of the power exchanged at the PCC (9), at each time interval, computed as the aggregation of net grid power of individuals $p_{n,t}$, (10).

$$\text{obj}: \min_{\boldsymbol{X_t}=\{x_{1,t},\ldots,x_{n,t}\}} F(\boldsymbol{X_t}) = \sum_{t \in T} \left(P_t\right)^2 \times dt \tag{9}$$

subject to:

$$P_t = \sum_{n \in N} p_{n,t} \quad = \sum_{n \in N} p^+_{n,t} - p^-_{n,t} \quad \forall t \in T \tag{10}$$

2.3. Household Objectives Scenarios

This section describes the operational objective at the end-user level. Different assumptions can be made, mostly depending on the considered pricing policy for the consumers. Typical approaches then consist in minimizing the energy bill about the purchase prices (time-dependent π^+_t) and the potential selling of electricity (fixed feed-in tariff π^-) – cost driven function f_n in (11).

$$\text{obj}: \min_{\mathbf{x_{n,t}} = \left\{ s^-_{n,t}, s^+_{n,t}, e_{n,t}, g^-_{n,t}, p^-_{n,t}, p^+_{n,t} \right\}} f_n(\mathbf{x_{n,t}}) = \sum_{t \in T} \left(p^+_{n,t} \times \pi^+_t - p^-_{n,t} \times \pi^-_t \right) \times dt \tag{11}$$

Three scenarios are investigated in this paper for the house operational strategy:

- **S1:** f_n with the time-of-use purchase price (day/night) and no possibility to curtail the generation (i.e. $g^-_{n,t} = 0$).
- **S2:** f_n with the time-of-use purchase price, and the possibility to curtail the generation.
- **S3:** f_n with the time-of-use purchase price, possibility to curtail the generation, and no feed-in tariff (i.e., $\pi^- = 0$).

As explained in the next section, users may not be willing to deviate from their local optimal solution in the course of the coordination strategy. Thus, an additional constraint is introduced at the house level for the day-ahead phase to represent the potential willingness of a user to respond to the coordinator's signals. This degree of response is computed as an acceptable deviation from the individual optimum (denoted f_n^0) with the coefficient α in (12).

$$\left| f_n(\mathbf{x_n}) - f_n^0(\mathbf{x_n}) \right| \leq \alpha \times f_n^0(\mathbf{x_n}) \tag{12}$$

3. Decentralized Optimization for Day-Ahead Commitment

3.1. Consensus Alternating Direction Method of Multipliers

Initially introduced in [15], ADMM has gained much interest in solving optimization problems in a distributed fashion. One typical ADMM variation consists of the determination of a consensus in a multi-agent environment (e.g., N agents with associated controls x_i) with convex objective functions (f_i) – derived from a global separable function. In (13), z_i denotes global variables that correspond to the expected system optimum, subject to potential constraints (not represented here). There is a need for consensus in the sense that different agents may compute different values for the same set of variables x_i based on their available information (expected match between x_i and z_i). Consensus ADMM (C-ADMM) then lies on the optimization of separated sub-problems inherited from the augmented Lagrangian of the original problem about the dual variables λ_i and with a convergence rate ρ (typically between 0 and 1), as expressed in (14).

$$\text{obj}: \min \sum_{i=1}^{i=N} f_i(x_i) \quad \text{s.t:} \quad x_i - z_i = 0 \tag{13}$$

$$L_i(x_i, \lambda_i, z) = f_i(x_i) + \lambda_i^T (x_i - z_i) + \frac{\rho}{2} \| x_i - z_i \|_2^2 \tag{14}$$

Table 2: C-ADMM algorithm

C-ADMM
Initialize : $\lambda_i = 0$, $z_i = 0$ **Repeat :** **1.** $x_i^{(k+1)} = \arg\min\ f_i(x_i) + \lambda_i^{(k)T}\left(x_i - z_i^{(k)}\right) + \rho/2\left\|x_i - z_i^{(k)}\right\|_2^2$ for $i = 1,..,N$ **2.** $z_i^{(k+1)} = \left\langle x_i^{(k+1)} \right\rangle$ - average over all agents **3.** $\lambda_i^{(k+1)} = \lambda_i^{(k)} + \rho/2\left(x_i^{(k+1)} - z_i^{(k+1)}\right)$ **Until** one stopping criterion is met

The algorithm then proceeds in iterations (upperscript $.^{(k)}$) with the optimization of the agent function (potentially subject to individual constraints) in step 1 and successive updates of the Lagrangian multipliers λ_i (step 3) and consensus variables (step 2) (refer to Table 2). The estimation of the consensus variables is the most important step in the coordination scheme and depends on the communication topology and the information exchanged between the different actors [7]. As an example, in typical ADMM for distributed optimal power flow, the voltage at a given node is a consensus variable, estimated as the average value of this voltage computed by all the neighboring electrical buses [16]. Typical stopping criteria can consist of a maximum number of iterations or sequences with no improvement of the objectives, or no significant changes in the variables values – i.e., primal residual $\left\|x_i^{(k)} - z_i^{(k)}\right\| < \varepsilon$ and/or dual residual $\left\|z_i^{(k)} - z_i^{(k-1)}\right\| < \varepsilon$.

3.2. Proposed Implementation

In this paper, C-ADMM is adapted to solve the considered problem in a decentralized way, starting with the sub-problem for every house *n*. The consensus values are denoted $\hat{p}_{n,t}$ in the agent problem (15) and relate to the grid power at the user meter level. Similarly to [17], the computation of the consensus value relies on an optimization problem solved by a coordination agent (e.g., at the PCC), once the controls are individually computed for each agent (all $p_{n,t}$ are then known). The goal is to minimize the Lagrangian function based on the original overall objective *F*, (16). Following the conventional last step of the ADMM iterations, multipliers are finally updated as expressed in (17).

$$\text{obj: } \min_{\boldsymbol{x_{n,t}}} f_n(\boldsymbol{x_{n,t}}) + \lambda_n^{\,T}\left(p_{n,t} - \hat{p}_{n,t}\right) + \frac{\rho}{2}\left\|p_{n,t} - \hat{p}_{n,t}\right\|_2^2 \tag{15}$$

$$\text{obj: } \min_{\substack{\hat{p}_{n,t} \\ \forall\{n,t\} \\ \in(N,T)}} F(\boldsymbol{X_t}) + \sum_{t\in T}\sum_{n\in N} \lambda_{n,t}^{\,T}\left(p_{n,t} - \hat{p}_{n,t}\right) + \frac{\rho}{2}\left\|p_{n,t} - \hat{p}_{n,t}\right\|_2^2 \tag{16}$$

$$\lambda_{n,t}^{(k+1)} = \lambda_{n,t}^{(k)} + \rho/2\left(p_{n,t}^{(k+1)} - \hat{p}_{n,t}^{(k+1)}\right) \tag{17}$$

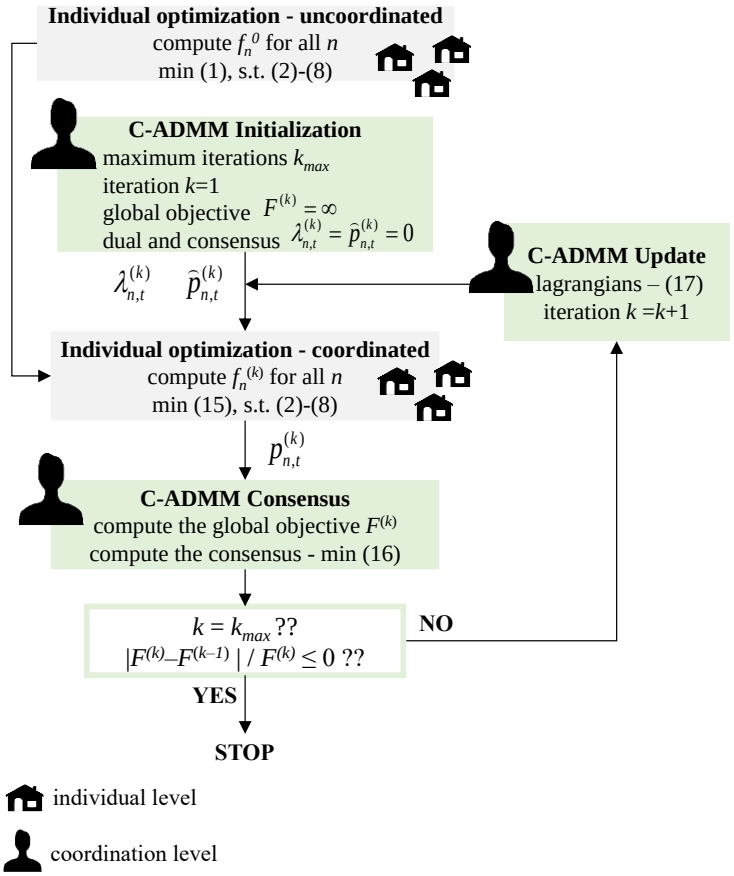

Figure 2: Implemented coordination strategy for day-ahead commitments on house grid power and aggregate profile at the coordinator level.

Ultimately, the adapted C-ADMM is implemented following the chart proposed in Figure 2 with successive optimizations over all the users and at the coordination level. The consumers communicate their expected grid power profile to the coordinator, who in turn updates the consensus and Lagrangian. At the user level, the consensus values can be interpreted as an optimal grid power profile to follow (requested by the coordinator). The Lagrangian value can be interpreted as the corresponding penalty (price signal). Finally, a stopping criterion of non-improvement of the global objective (< 1%) is considered in addition to the maximum number of iterations.

4. Three-step Strategy for Real-time Operations

The day-ahead phase returns committed grid profiles at the households level $p_{n,t}^{da}$ along with an optimal trajectory for the battery state of charge $soc_{n,t}^{da}$. Similarly, the profile expected for the next day at the PCC level is obtained and denoted $P_{n,t}^{da}$. In real-time, due to a finer time resolution and unavoidable prediction errors, the controls need to be adjusted to fulfill the day-ahead commitments as much as possible. As previously, those adjustments shall rely on an efficient and fast coordination strategy at every time step. In the notations, the time index t indiscriminately refers to the day-ahead resolution (30 min) and the real-time discretization (5 min). In practice, two temporal sets are mathematically introduced along with sampling and mapping between the two resolutions to identify the corresponding *da* time step at a given *rt* instant. Those two distinct sets are not explicit here for the sake of simplicity. To control the computational time and avoid multiple iterations in the coordination process, a simple strategy is considered here with a convergence guaranteed at every time step in the real-time phase. It consists of three main steps described in the following subsections.

4.1. Step 1: Characterize and Declare Household Capabilities

In this first step, each house computes the potential values of the grid power at the meter level it can reach for a given time step considering the actual load and generation conditions. By default, the real-time objective at the household level is to remain as close as possible to its committed profile. $p_{n,t}^{rt\ 0}$ denotes the household grid power in real-time considering the actual load value $l_{n,t}^{rt}$ and available solar generation and computed while applying the controls calculated in the day-ahead phase for the corresponding time step (i.e., battery charge/discharge and generation curtailment) ((18)). Obviously, in real-time, it is not possible to curtail more than the actual, available generation.

$$p_{n,t}^{rt\ 0} = l_{n,t}^{rt} + g_{n,t}^{0rt} - \underbrace{s_{n,t}^{-da} + s_{n,t}^{+da} - \min\left(g_{n,t}^{-da}, g_{n,t}^{0rt}\right)}_{\text{avalaible from the day-ahead phase}} \tag{18}$$

For given solar generation and load, every user can modulate the power it draws/inject from/to the grid while adjusting the storage power setpoints and thus mitigate uncertainties is real time. However, any battery usage to cope with real-time adjustments incurs deviations about the predicted state of charge trajectory at the next time step. Thus, any over solicitations of the storage equipment to mitigate uncertainties may endanger the capability to absorb a local energy surplus or compensate any deficit in future time steps. Therefore, a bandwidth is defined around the predicted state of charge trajectory with a tolerance Δsoc and an additional operating constraint (19). Ultimately, that bandwidth can be considered in an optimal dispatch for near real time control that compute the best potential grid power value for each user – i.e. minimizing the distance with the user day-ahead reference while considering the generic system constraints of section 2 ((20)). Note that equation (4) on energy limits can still be considered. Ultimately, only the strictest values are 'mathematically active' – i.e. considered in the solving phase.

$$\max\left(\underline{soc}, soc_{t+1}^{da} + \Delta soc\right) \leq soc_{t+1} \leq \min\left(\overline{soc}, soc_{t+1}^{da} + \Delta soc\right) \tag{19}$$

$$p_{n,t}^{rt\ *} = \underset{x_{n,t}}{\arg\min}\left(p_{n,t} - p_{n,t}^{da}\right)^2 \quad \text{s.t. (2)-(8) \& (19)} \tag{20}$$

At this stage, it is also possible to compute the extreme (min/max) grid values reachable by each household for measured solar and load levels while accounting for the storage and curtailment capabilities. Similar to the best reachable values, the potential maximum grid power, $\overline{p_{n,t}^{rt}}$ and the minimum $\underline{p_{n,t}^{rt}}$ can be obtained while solving an optimization problem (21), considering the generic constraints along with the *soc* tolerance (19). In addition, and similarly to the day-ahead phase, users may be more or less willing to deviate from their estimated optimum grid power value in real-time. Thus, when computing the potential min/max values, an additional constraint can be considered to account for the user's willingness to participate in the real-time coordination – similar coefficient as in the day-ahead phase ((22))

$$\begin{cases} \underline{p_{n,t}^{rt}} = \underset{x_{n,t}}{\arg\min}\left(p_{n,t}\right) \\ \overline{p_{n,t}^{rt}} = \underset{x_{n,t}}{\arg\min}\left(-p_{n,t}\right) \end{cases} \quad \text{s.t. (2)-(8) \& (19)} \tag{21}$$

$$\left|p_{n,t} - p_{n,t}^{rt\ *}\right| \leq \alpha \times p_{n,t}^{rt\ *} \tag{22}$$

4.2. Step 2: Compute Household Reference Power at the Coordinator Level

The available/reachable grid power values computed at each household level are then forwarded to the coordinator. Based on those values, the coordinator computes the most appropriate references in terms of

users' grid power to be as close as possible to the aggregated profile committed in day-ahead P_t^{da} . This optimization accounts for the minimum and maximum grid values declared by the households and tries to limit the deviations with their best values ((23)).

$$p_{n,t}^{rt} = \underset{\substack{\underline{p_{n,t}^{rt}} \le p_{n,t} \le \overline{p_{n,t}^{rt}} \\ \forall n \in N}}{\arg\min} \left(\left(\sum_{n \in N} p_{n,t} - P_t^{da} \right)^2 - \sum_{n \in N} \left(p_{n,t} - p_{n,t}^{rt\,*} \right)^2 \right) \tag{23}$$

This coordination phase at the central level is necessary as a case where each household meets its best value (grid power value closer to the one predicted in day-ahead) cannot ensure the best performance at the PCC level, once all the profiles are aggregated. This will be discussed in the results section. More specifically, the performances with and without real-time adjustment and coordination will be compared.

4.3. Step 3: Perform the Control

The reference grid power values are then sent back to each household before they control their assets in real-time ($\boldsymbol{x_{n,t}}$) to meet the desired value $p_{n,t}^{rt}$. Those controls are subject to generic household constraints.

$$obj: \min_{\boldsymbol{x_{n,t}}} \left(p_{n,t} - p_{n,t}^{rt} \right)^2 \quad \text{s.t. (2)-(8) \& (19)} \tag{24}$$

The overall three stage strategy for real-time coordination is finally summarized in Figure 3 with the information exchanged over the different steps and the corresponding problems solved to compute the grid power values. Ultimately the convergence of step 3 is ensured as the operating points, in terms of grid power values, account for the household capabilities in real-time given the instantaneous actual values of the load and the available generation (coming from the optimization on step 1). Also, the value of the state of charge is updated at every time step in real-time about the actual storage controls. Finally, and as discussed in the next section, extracting the best value at the household level ($p_{n,t}^{rt\,*}$) allows highlighting the need for coordination and comparing the overall system performances with the actual controls ($p_{n,t}^{rt}$).

Note that the three steps introduced rely on optimization. For simulation purposes and/or improved simplicity and explainability, those steps could be replaced by heuristics while solving the problems with sets of predefined rules. In particular, this could reduce the need for computational capabilities in real time at the user levels – i.e. constrained optimization problems to solve at the level of every users. Investigating heuristics to replace the aforementioned problems is beyond the scope of the paper.

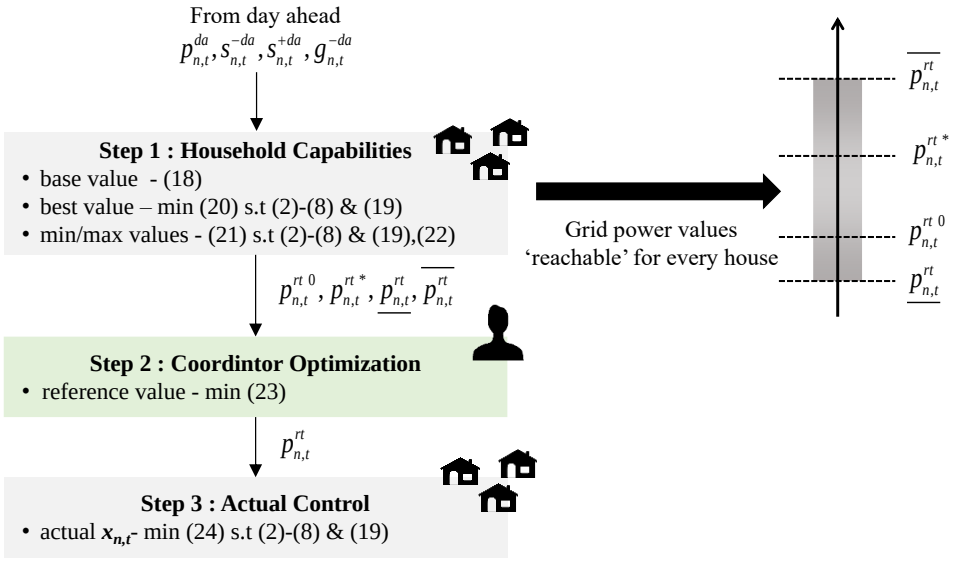

Figure 3: Real-time management strategy and exchanged information in terms of grid power ('meter') at the household level.

5. Obtained Results

For the simulations provided in this section, the different load profiles are taken from the REFIT data set [18], and the solar generation is computed with radiation profiles from NASA open data[1]. All the implemented problems in both day-ahead and real-time phases are implemented using the YALMIP toolkit [19] in MATLAB 2018b and solved with CPLEX 12.10.0.

5.1. Day-Ahead Commitment

5.1.1. Preliminary Test with Three Houses

The first set of simulations is run with three houses equipped with a 6 kWp solar generator and a 2 kW/kWh storage system. Figure 4*a* displays the aggregated grid profiles (e.g., at the PCC level) along the simulated day. With no control ability for storage and curtailment (i.e., "no scontrol") the net power profile leads to significant back-feed power – global objective value F = 163 kWh2. In that case, the grid power profile is merely the aggregated load minus generation profile. When users individually control (i.e. "uncoordinated control") their storage, the reverse power remains significant as the consumers benefit from the feed-in tariff in the first scenario (**S1**). Also, this cost-driven optimization leads to a significant night peak in the overall imported power due to uncoordinated storage charge (F = 123 kWh^2.). The global optimum corresponds to a case where the coordinator can directly control the assets 'behind the meter'. The back-feed power is then smoothed as much as possible for the lowest objective value of F = 58 kWh^2.

[1] https://power.larc.nasa.gov

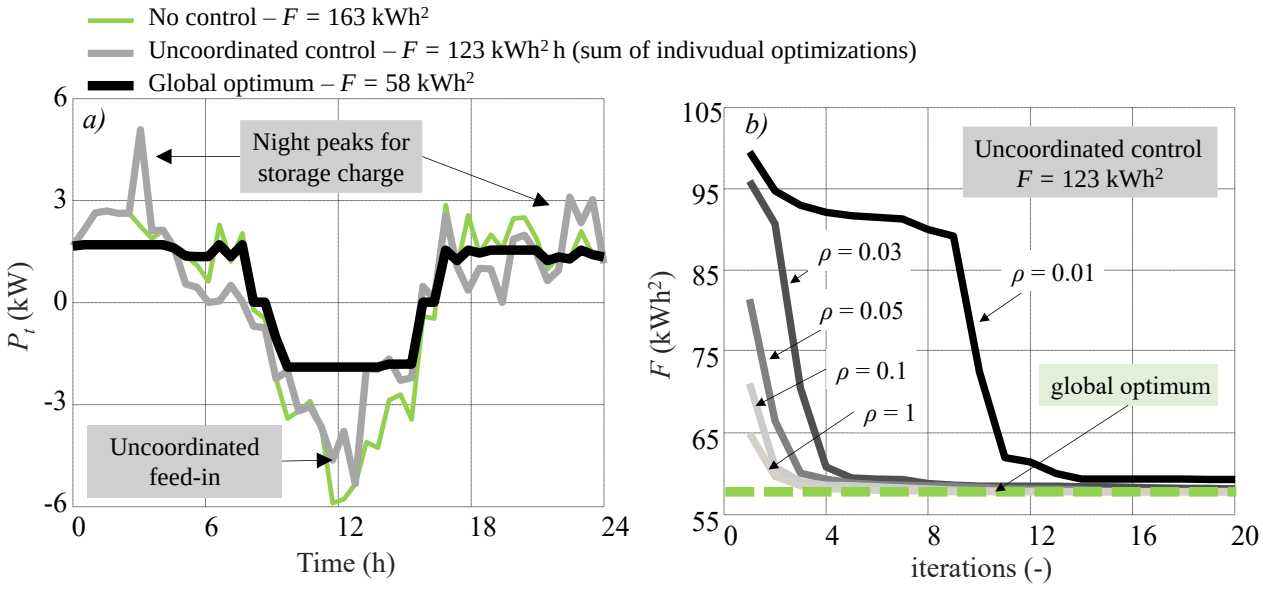

Figure 4: *a*) Aggregated grid power – global optimum and solution with no storage or uncoordinated storage control. *b*) Global objective decrease along the iterations for different convergence rate values.

Running the proposed collaboration scheme for the three houses system allows to reduce the global objective value over the algorithm iterations compared to uncoordinated control – when all the houses agree to deviate from their optimum (i.e., $\alpha = 1$). Preliminary tests show that increasing the convergence rate fastens the convergence (four iterations for $\rho = 1$), which is not systematic for that class of coordination problem (Figure 4*b*). Especially with greater convergence rate values, the global objectives decreases significantly at the first iteration. At that iteration and for the case study considered here last term of the augmented Lagrangian in (16) corresponds to the global objective (minimum of square grid power $F(\boldsymbol{X}_t)$) - with an optimum corresponding to the initial value of the consensus variables (set to 0). The convergence rate remains fixed to unity in the following simulations. Additional runs consist in setting the user preferences in terms of response to coordinator signals. Figure 5*a* displays the algorithm convergence with the global objective optimal value that cannot be met in the case of non-fully responsive customers (i.e. α <1). Note that for $\alpha = 0$, houses do not degrade their performances (Figure 5*b*), but the overall objective F can still be improved compared to a case with uncoordinated control (F = 99 kWh²).

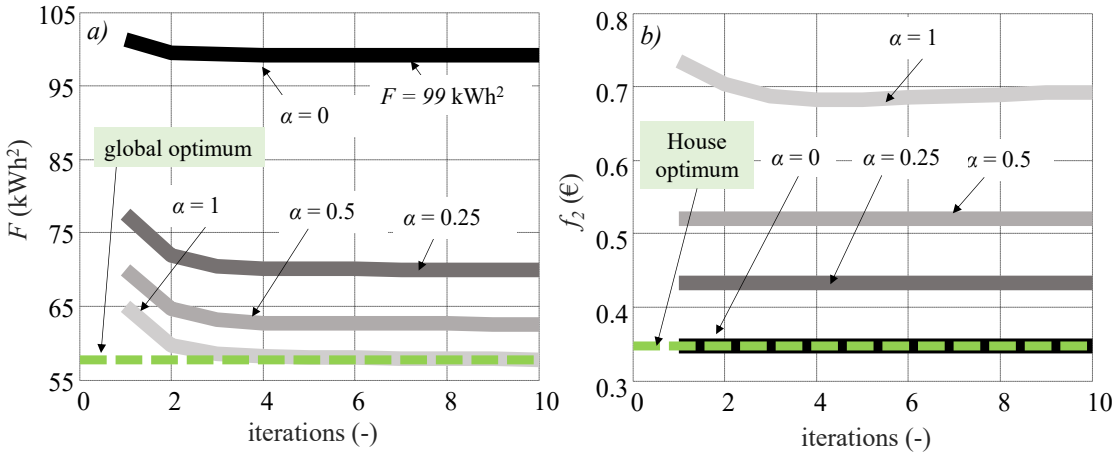

Figure 5: Objectives values for different α settings – *a)* global and *b*) individual (house 2).

The loss of benefit (or increased cost) of the user depends on the considered billing/control scenario. Table 3 gives the objective values of the individual house and PCC in case of uncoordinated control (upperscript $.^0$) and once the proposed strategy is run (upperscript $.^*$). As previously observed for scenario **S1**, the coordination strategy improves the global objective (for the aggregated power) at the cost of slightly increased energy bills of the three houses ($\alpha = 1$). In scenario **S2**, in which the ability to curtail part or all the generation is considered, this additional degree of freedom allows us to reach a better value of the global objective with reduced back-feed power at the PCC level. This curtailment at the house level that responds to coordination signals directly leads to a loss of revenue, which is reduced when no feed-in tariff is considered (scenario **S3)**.

Table 3: Global and users objectives values for different scenarios

	F^0	F^*	f_1^0	f_1^*	f_2^0	f_2^*	f_3^0	f_3^*
S1	123	58	–0.3	–0.1	0.3	0.7	1.7	2.0
S2	123	36	–0.3	0.6	0.3	1.1	1.7	2.2
S3	119	36	0.7	0.7	1.1	1.2	2.1	2.2

5.1.2. Scalability to 100 Houses

Preliminary scalability tests consist in increasing the size of the controlled community to 100 houses. Results, not displayed here, showed that the coordination strategy converged in four to six iterations in all cases and for the three pricing scenarios (**S1, S2, S3**). The set of households is then fixed to 100 and additional tests are performed with increasing numbers of coordinated houses – while the others remain controlled individually. Figure 6 displays the total loss of revenue (over all the houses) and the global objective F values. For the first scenario, the optimum of the global objective is out of reach with the impossibility to curtail the generation at the house level. Both the decrease of F and the increase of the energy bill evolve almost linearly with the number of coordinated houses (Figure 6*a*). The loss of revenue is much higher in **S2** with the curtailed generation not sold. However, when the number of coordinated houses increases, the loss of revenue tends to be reduced thanks to the spread effect of more heterogeneous profiles (Figure 6*b*) [20]. The same observation can be made in S3 with a lower loss of revenue – no feed-in tariffs (Figure 6*c*).

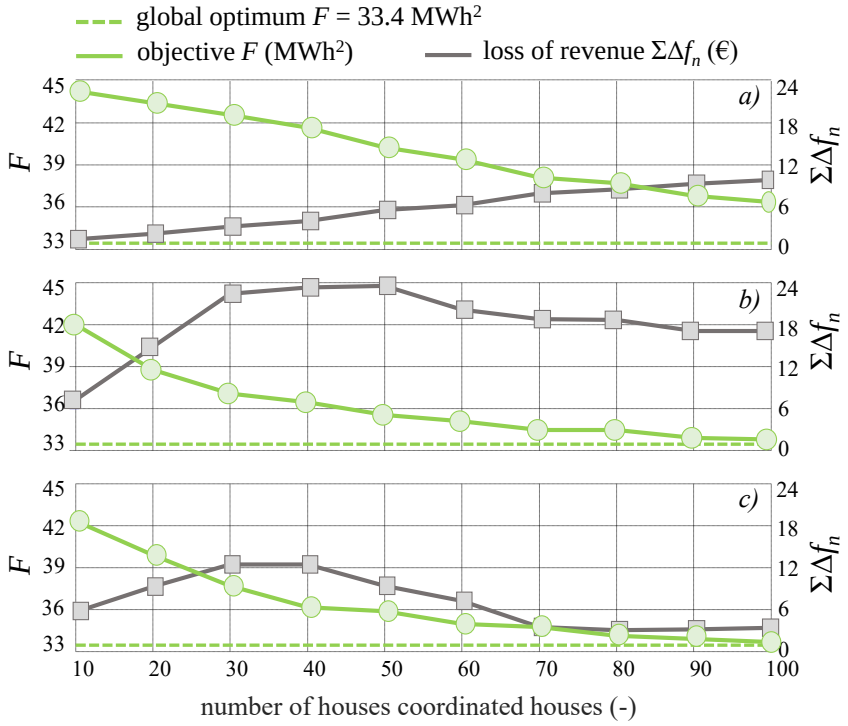

Figure 6: Objective and loss of revenue for different numbers of coordinated houses – *a*) S1, *b*) S2, *c*) S3.

Another set of simulations for **S2** consists of increasing the number of coordinated houses for different settings α. One interesting result of Figure 7 is that some improvements to the global objective can still be achieved without degrading the individual objective when $\alpha = 0$ ('free' coordination). Global performance increases with greater values. In that case, the optimal value is reached only when all the houses coordinate together.

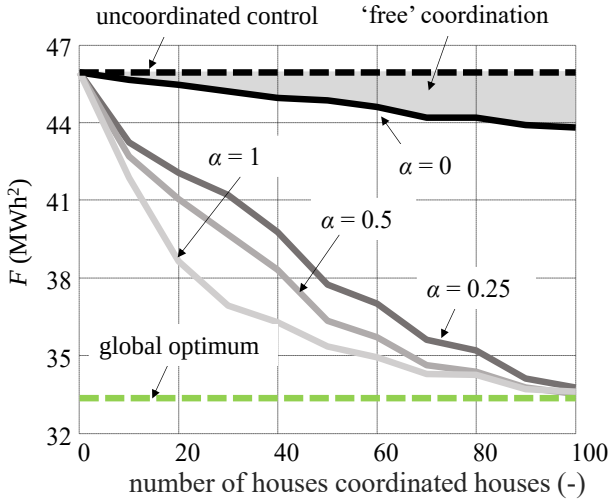

Figure 7: Global objective for different numbers of coordinated houses (out of 100 users) and willingness to respond to coordination signals.

5.2. Real-Time Control

5.2.1. Preliminary Test with Three Houses

In this section, the performances of the real-time operations are assessed in terms of deviations of the aggregated power profile (in real-time at the coordinator/PCC level) with the profile committed in day-ahead – error in terms of Energy Deviation (*ED* in %) between the overall actual power profile and the one predicted in the day-ahead phase P_t^{da} as expressed in (25). Similarly, the total energy within the measured deviation ED^{TOT} in kWh is computed with (26) as a supplementary metric. Also note that those metrics can assessed with different real-time solutions - i.e., without any adaptation of the scheduled controls ($p_{n,t}^{rt\ 0}$), with the optimization at the household level only ($p_{n,t}^{rt\ *}$), and with the proposed three-step coordination ($p_{n,t}^{rt}$).

$$ED = \frac{1}{\|T\|} \times \sum_{t \in T} \frac{\left| P_t^{da} - P_t^{rt} \right| \times dt}{\left| P_t^{da} \right| \times dt} \times 100 \tag{25}$$

$$ED^{TOT} = \sum_{t \in T} \left| P_t^{da} - P_t^{rt} \right| \times dt \tag{26}$$

The first set of simulations is performed with three houses operated following the first scenario **S1** – (i.e., no possibility to curtail the generation). In the absence of historical forecast, the method in the Appendix is proposed in order to generate prediction profile form actual measurements. Especially, a parameter allows to set the expected forecast error, for sensitivity analysis that is furtherly discussed. At first, forecast errors of 30 % are considered with day-ahead predictions for the load and generation (at a 30 min resolution) computed with a half-hourly average of real-time profiles (at a 5 min resolution). Figure 8*a* displays the results that would be obtained regarding the overall power profile at the coordinator/PCC level, with no adaptation of the scheduled controls (*ED* = 11 %). When users individually optimize their controls to fulfill their own schedule grid power commitment, the error decrease to 10 %. The proposed coordination further decreases the energy deviations around the committed profile (*ED* = 7 %) while optimizing the household control within their capabilities at every time step (Figure 8*b*).

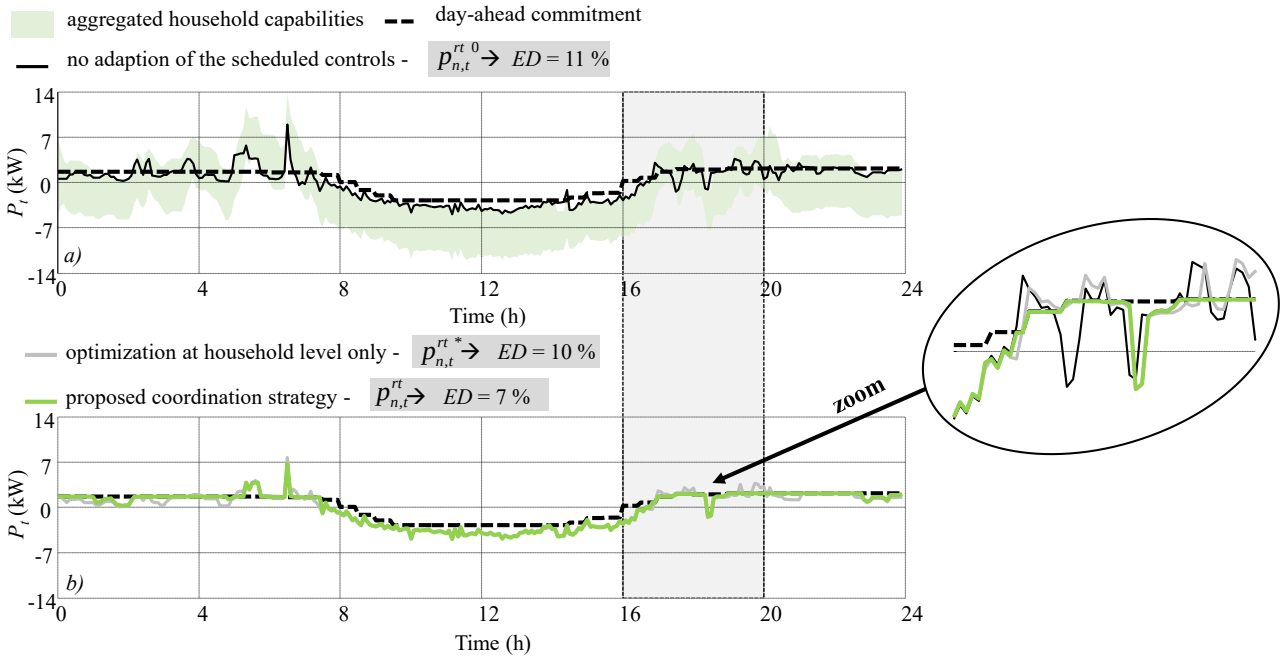

Figure 8: Aggregated power profile at the coordinator level after real-time operations – *a)* household capabilities and results with no correction of the scheduled controls – *b)* results with individual and coordinated optimization.

Figure 9a illustrates the results at the level of a single household in terms of grid power profile and the state of charge is depicted in Figure 9b after running the two stages of the proposed management strategy – i.e. look ahead phase and near real time correction. For the simulated day, the coordination strategy globally leads to an overcharge of the storage compared to the scheduled profiles. Consequently, the household tends to increase its grid power value to compensate for an overall surplus of generation (compared to the forecast) at the global level. Note that the surplus of solar injection cannot be avoided here as the possibility to curtail is not considered (scenario **S1**).

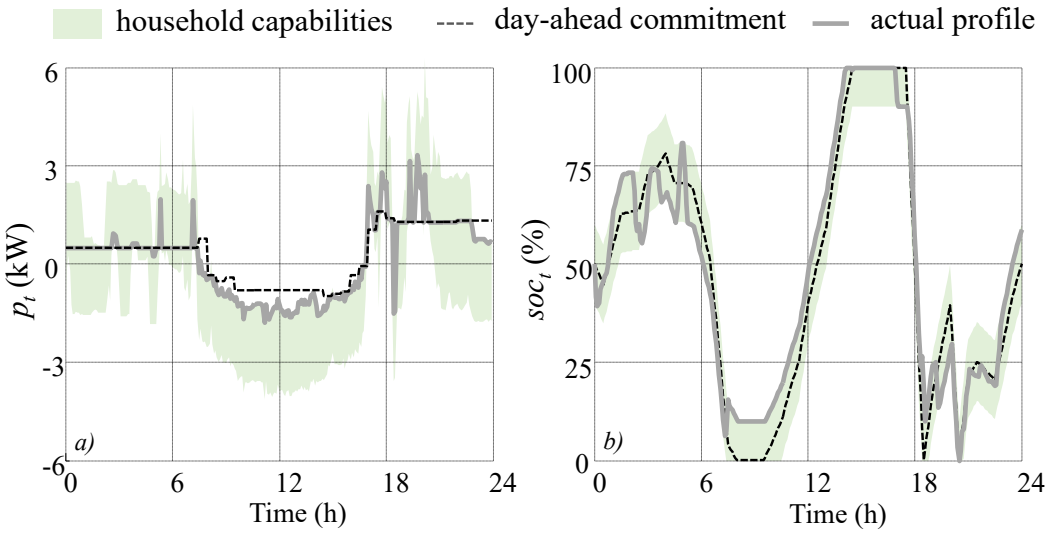

Figure 9: Real-time operations at the household level – *a)* grid power profile – *b)* storage state of charge.

5.2.2. Impact of Forecast Uncertainties and Storage Parameters

The previous simulations were carried out with a set of forecasted load and generation profiles that displayed a 30 % error from the actual real-time power profiles. Additional tests are here performed while generating several sets of forecasts from single real-time profiles for the households' load and solar generation. Those predictions are generated to reach custom error with the real-time values (in terms of normalized RMSE) with the formulation of the optimization problem explicated in the Appendix. The error in terms of Energy Deviations (*ED*) is then computed for sets of forecasts. As previously, different real-time solutions can be considered: without any adaptation of the scheduled controls ($p_{n,t}^{rt\,0}$), with the optimization at the household level ($p_{n,t}^{rt\,*}$), and with the proposed three-step coordination ($p_{n,t}^{rt}$).

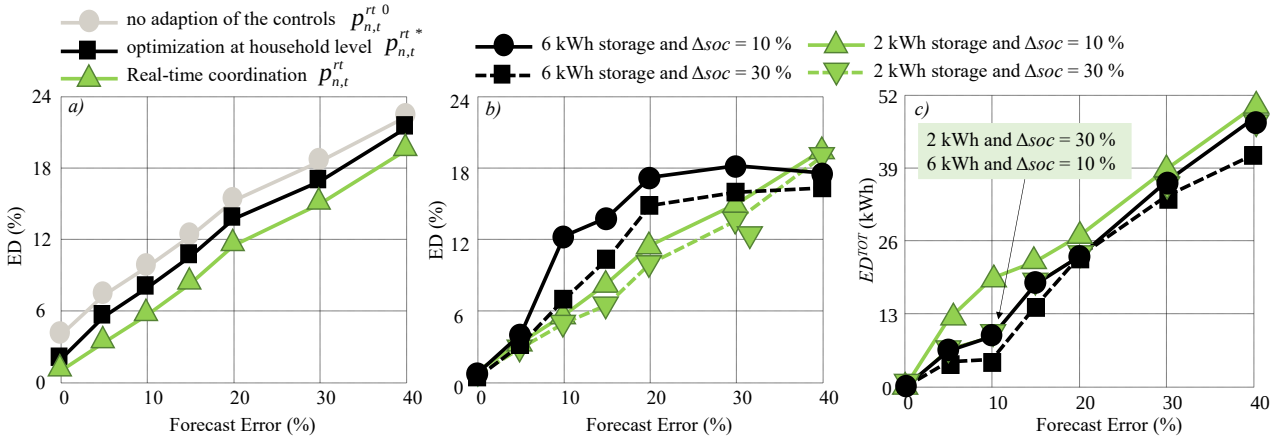

Figure 10: Impact of forecast error – *a)* uncoordinated Vs coordinated households – *b)* energy deviation in % (ED) for coordinated households with different storage parameters – *c)* energy deviation in kWh (ED^{TOT}) for coordinated households with different storage parameters.

Results displayed in Figure 10*a* show that, as can be expected, ED values tend to increase with greater forecast errors, almost linearly. Similar to the previous section, the results highlight the need for coordination to lower the *ED* values and remain as close as possible to the predicted profile at the global level. Note that with no forecast error, the deviation with the predicted profile is not null. This is due to the different time resolution adopted for the two phases with potential high-power oscillations in the real-time profiles. It is noticeable that the ED improvement provided by the coordination remains somewhat constant no matter the forecast error values (around a 2-3 % improvement compared to a case with no coordination). Indeed, if the proposed strategy allows to better satisfy the day-ahead commitment, at the first order, the performances in terms of errors (ED) depend on the look-ahead profile itself. Thus, similar tests are performed for different storage sizes (2 kWh and 6 kWh wit the rated power fixed at 2 kW) while increasing the state of charge bandwidth (Δsoc = 10 % or 30 %). Figure 10*b* displays the results. Unexpectedly, increasing the storage capacity does not reduce the deviations between the predicted profiles and the actual one, once the real-time coordination is performed. This is because bigger storage capacities imply a more significant impact on the predicted look-ahead profiles (e.g., a smoother power profile at the coordinator level), and more corrective actions may be required in real-time to mitigate the forecast errors. Also, to energy deviation metric in % may be misleading in such cases as the reference day-ahead grid power profiles displays values closer to 0 (i.e. smoother profile). Figure 10*c* displays the same results according to the absolute energy deviation metric (ED^{TOT}) and the 6kWh case study displays lower deviations as could be expected. It is also interesting to note that, on average, a 6kWh storage with a soc allowance of 10 % return the same results as a 2kWh battery with a soc deviation tolerance of 30 % - in terms of energy deviations in real time and for different forecast quality. Additional tests could be performed while disaggregating the storage capacity, as a usable capacity for the look-ahead phase (e.g., 50 % of the nominal storage size), and allow more flexibility for the real-time operation depending on the expected forecast errors. This is outside the scope of the paper.

5.2.3. Scalability to 100 Houses

A last set of simulations is performed while increasing the number of coordinated houses for both look-ahead and real-time phases. As previously, tests are run with different assumptions on the forecast errors. Results in Figure 11*a* show that the forecast error has a great impact on the system's performance. As for the look-ahead stage results, increasing the number of coordinated houses reduces the global objective (i.e., smoothens the power profile at the PCC level). However, with greater forecast deviations, the scheduled policy leads to predicted grid profiles that display too many discrepancies with actual values, and the best objective values cannot be reached. As previously, the error between the actual and predicted profile increases with the

forecast error (Figure 11*B*). In addition, it is also noticeable that the error with the committed profiles is somewhat constant no matter the number of coordinated houses (except with 80 houses where the added users display great solar capacities compared to the installed storage). Ultimately, those results, as the previous ones, highlight the need for a tradeoff between the targeted objective in the look-ahead phase, and the confidence that it can be fulfilled in real-time.

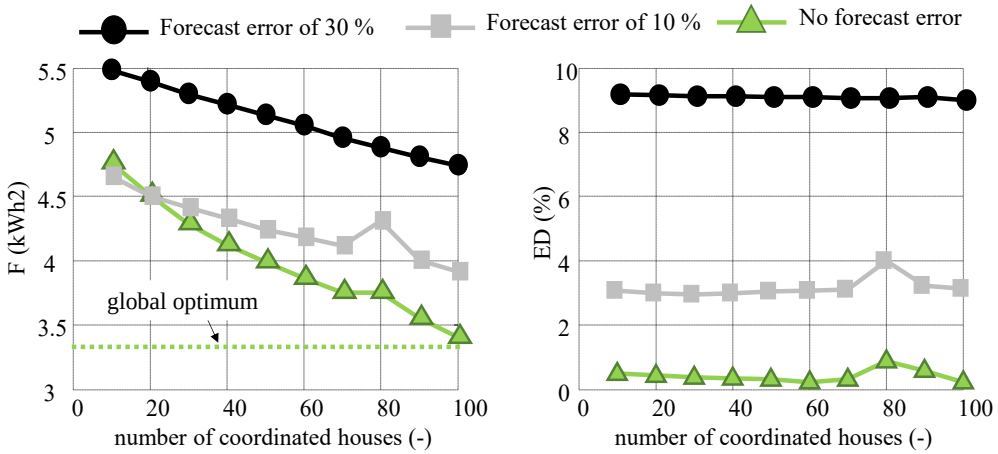

Figure 11: Increased numbers of coordinated houses with different forecast errors – *a)* global objective value after real-time operations – *b)* errors with profiles committed in the look-ahead phase.

6. Conclusions

This paper successfully implemented a coordination strategy to control storage units 'behind the meter'. The strategy lies in a two-stage approach with look-ahead commitments (daily) followed by an online adaptation of the controls to remain as close as possible to the predicted profiles. Performances are assessed in terms of aggregated power profiles at the coordinator level with smooth patterns and the error between actual profiles and committed values. Scalability tests up to a hundred coordinated households were performed, along with the impact study of the forecast errors and end-users' settings. For the look ahead phase, the obtained results show that the coordination allows reaching the system optimality when end-users are willing to participate. Also, some improvements at the global scale can still be achieved without degrading the individual energy bills. The last simulations showed that the more users, the less they need to decrease their economical performances to reach the same system performances. Such tests with a trade-off between individual and global objectives can be of use to price/incentivize the response of the user in terms of services provided to the community.

The results of the real-time phase highlighted the need for an online adaptation of the controls to fulfill the look ahead commitment as much as possible. Convergence of the real-time phase was ensured in all the investigated scenarios with a proposed three-step procedure with household controls based on their capabilities updated at each time step. Especially, results showed that errors between predicted and actual profiles are not necessarily lowered with increased storage sizes or a greater number of coordinated houses. In such cases, more flexibility capacity is available in the look-ahead phase to reach a better value of the global objectives while controlling the equipment between their bounds (e.g., the storage state of charge). However, this does not ensure the storage to be able to mitigate efficiently forecast errors in cases they already reached their limits. Thus, a trade-off shall be found between the use of storage capacities to 'modulate' the grid profiles in the look-ahead phase, and the need for uncertainties mitigation. One possibility could be to allocate only a limited part of a storage capacity to the look-ahead scheduling, while the whole available energy may be used in real-time. This will be part of future works that shall also investigate the introduction of grid constraints. Especially,

in the real-time phase, the computation at the coordinator level shall account for voltage/current limitations while generating the controls for each individual end-user within its capabilities.

7. Acknowledgment

The work has been carried out in the framework of the AI4DG project – Artificial Intelligence for Distribution Grids, a French-German initiative co-funded by ANR and BMBF.

8. Appendix

This appendix describes the method proposed to generate different sets of forecasts x_t^{da} with predefined errors from a given real-time profile x_t^{rt}. Similar to the paper and for the sake of simplicity, the distinction between look ahead and the real-time temporal set is not explicated. Here the time index refers to the temporal resolution of the prediction. The forecast generation is then formulated as an optimization problem. The objective is to optimize the profile predicted on the day ahead with a minimum distance compared to the reference real-time profile ((27)). The second term in the objective aims at limiting the oscillations of the generated profile with a penalty coefficient λ. Such oscillations may not be realistic for forecasts and can occur when predictions are usually generated using random noise – e.g., normal law around given profiles [9]. The predictions are generated to reach custom error with the real-time values (in terms of normalized RMSE) with a predefined $nRMSE_c$ in constraint (28). Another constraint is introduced to further limit the oscillations of the generated profiles, while controlling the amount of deviation 'above' and 'below' the reference real-time values with a predefined tolerance ψ coefficient in (29). Specific attention is attached to the upper bounds for the generated profile x_t^{da}. While the lower bounds remain null, the predicted values shall not exceed too much the reference real-time values (multiplication factor φ in (30)). In the case of the solar generation forecast, the predicted profile cannot exceed clean sky values (i.e., with no clouds denoted $\overline{x_t^{rt}}$ in (30)) for the corresponding day and given geographical locations [21].

$$ob: \min_{x_t^{da}} \left(\sum_{t \in T} \left(x_t^{da} - x_t^{rt} \right)^2 + \lambda \times \sum_{t \in T - \{||T||\}} \left| x_{t+1}^{da} - x_t^{da} \right| \right) \tag{27}$$

$$nRMSE = \frac{\sqrt{\sum_{t \in T} \left(x_t^{da} - x_t^{rt} \right)^2}}{\left\langle x_t^{rt} \right\rangle} = nRMSE_c \tag{28}$$

$$\left(\sum_{t \in T} \max\left(x_t^{rt} - x_t^{da}, 0 \right) - \sum_{t \in T} \left| \min\left(x_t^{rt} - x_t^{da}, 0 \right) \right| \right)^2 \leq \psi \tag{29}$$

$$\begin{cases} 0 \leq x_t^{da} \leq \varphi \times x_t^{rt} & \text{for load profiles} \\ 0 \leq x_t^{da} \leq \min\left(\varphi \times x_t^{rt}, \overline{x_t^{rt}} \right) & \text{for solar generation profiles} \end{cases} \tag{30}$$

Figure 12 gives both load and solar generation forecasts as an illustrative example with different nRMSE values around given real-time values (at the look-ahead resolution of 30 min here).

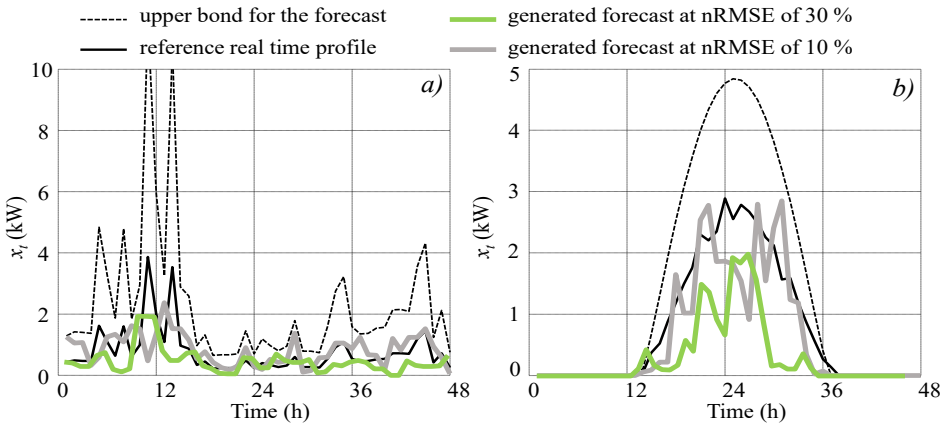

Figure 12: Illustrative generated forecast based on reference real-time profiles – *a)* load profile – *b)* solar generation profiles.

9. References

[1] P. D. Lund, J. Lindgren, J. Mikkola, and J. Salpakari, 'Review of energy system flexibility measures to enable high levels of variable renewable electricity', *Renew. Sustain. Energy Rev.*, vol. 45, pp. 785–807, May 2015, doi: 10.1016/j.rser.2015.01.057.

[2] Z. Li, X. Wang, D. Lin, R. Zheng, B. Han, and G. Li, 'Smart energy management model for households considering incentive-based demand response', in *2021 Power System and Green Energy Conference (PSGEC)*, Aug. 2021, pp. 327–332. doi: 10.1109/PSGEC51302.2021.9541695.

[3] R. Carli and M. Dotoli, 'Cooperative Distributed Control for the Energy Scheduling of Smart Homes with Shared Energy Storage and Renewable Energy Source', *IFAC-Pap.*, vol. 50, no. 1, pp. 8867–8872, Jul. 2017, doi: 10.1016/j.ifacol.2017.08.1544.

[4] C. Berk, R. Roche, D. Bouquain, and A. Miraoui, 'Decentralized Neighborhood Energy Management With Coordinated Smart Home Energy Sharing', *IEEE Trans. Smart Grid*, vol. 9, no. 6, pp. 6387–6397, 2018.

[5] C. Ruiz, A. J. Conejo, J. D. Fuller, S. A. Gabriel, and B. F. Hobbs, 'A tutorial review of complementarity models for decision-making in energy markets', *EURO J. Decis. Process.*, vol. 2, no. 1–2, pp. 91–120, Jun. 2014, doi: 10.1007/s40070-013-0019-0.

[6] P. Yu, C. Wan, Y. Song, and Y. Jiang, 'Distributed Control of Multi-Energy Storage Systems for Voltage Regulation in Distribution Networks: A Back-and-Forth Communication Framework', *IEEE Trans. Smart Grid*, vol. 12, no. 3, pp. 1964–1977, May 2021, doi: 10.1109/TSG.2020.3026930.

[7] F. Etedadi Aliabadi, K. Agbossou, S. Kelouwani, N. Henao, and S. S. Hosseini, 'Coordination of Smart Home Energy Management Systems in Neighborhood Areas: A Systematic Review', *IEEE Access*, vol. 9, pp. 36417–36443, 2021, doi: 10.1109/ACCESS.2021.3061995.

[8] Y. Chen, C. Deng, D. Li, and M. Chen, 'Quantifying cumulative effects of stochastic forecast errors of renewable energy generation on energy storage SOC and application of Hybrid-MPC approach to microgrid', *Int. J. Electr. Power Energy Syst.*, vol. 117, p. 105710, May 2020, doi: 10.1016/j.ijepes.2019.105710.

[9] W.-J. Ma, J. Wang, V. Gupta, and C. Chen, 'Distributed Energy Management for Networked Microgrids Using Online ADMM With Regret', *IEEE Trans. Smart Grid*, vol. 9, no. 2, pp. 847–856, Mar. 2018, doi: 10.1109/TSG.2016.2569604.

[10] M. A. Putratama, R. Rigo-Mariani, A. D. Mustika, V. Debusschere, A. Pachurka, and Y. Bésanger, 'A Three-Stage Strategy with Settlement for an Energy Community Management Under Grid Constraints', *IEEE Trans. Smart Grid*, pp. 1–1, 2022, doi: 10.1109/TSG.2022.3167862.

[11] J. Silva *et al.*, 'Estimating the Active and Reactive Power Flexibility Area at the TSO-DSO Interface', *IEEE Trans. Power Syst.*, vol. 33, no. 5, pp. 4741–4750, Sep. 2018, doi: 10.1109/TPWRS.2018.2805765.

[12] Y. Ding, Q. Xu, Y. Xia, J. Zhao, X. Yuan, and J. Yin, 'Optimal dispatching strategy for user-side integrated energy system considering multiservice of energy storage', *Int. J. Electr. Power Energy Syst.*, vol. 129, p. 106810, Jul. 2021, doi: 10.1016/j.ijepes.2021.106810.

[13] O. M. Akeyo, V. Rallabandi, N. Jewell, and D. M. Ionel, 'The Design and Analysis of Large Solar PV Farm Configurations With DC-Connected Battery Systems', *IEEE Trans. Ind. Appl.*, vol. 56, no. 3, pp. 2903–2912, May 2020, doi: 10.1109/TIA.2020.2969102.

[14] B. Gao, X. Liu, C. Wu, and Y. Tang, 'Game-theoretic energy management with storage capacity optimization in the smart grids', *J. Mod. Power Syst. Clean Energy*, vol. 6, no. 4, pp. 656–667, Jul. 2018, doi: 10.1007/s40565-017-0364-2.

[15] S. Boyd, 'Distributed Optimization and Statistical Learning via the Alternating Direction Method of Multipliers', *Found. Trends® Mach. Learn.*, vol. 3, no. 1, pp. 1–122, 2010, doi: 10.1561/2200000016.

[16] M. A. Putratama, R. Rigo-Mariani, V. Debusschere, and Y. Besanger, 'Parameter Tuning for LV Centralized and Distributed Voltage Control with High PV Production', in *2021 IEEE Madrid PowerTech*, Jun. 2021, pp. 1–6. doi: 10.1109/PowerTech46648.2021.9494802.

[17] T. Morstyn and M. D. McCulloch, 'Multiclass Energy Management for Peer-to-Peer Energy Trading Driven by Prosumer Preferences', *IEEE Trans. Power Syst.*, vol. 34, no. 5, pp. 4005–4014, Sep. 2019, doi: 10.1109/TPWRS.2018.2834472.

[18] T. Kane, S. K. Firth, T. M. Hassan, and V. Dimitriou, 'Heating behaviour in English homes: An assessment of indirect calculation methods', *Energy Build.*, vol. 148, pp. 89–105, Aug. 2017, doi: 10.1016/j.enbuild.2017.04.059.

[19] J. Lofberg, 'YALMIP : a toolbox for modeling and optimization in MATLAB', in *2004 IEEE International Conference on Robotics and Automation (IEEE Cat. No.04CH37508)*, Sep. 2004, pp. 284–289. doi: 10.1109/CACSD.2004.1393890.

[20] A.-L. Klingler, 'Self-consumption with PV+Battery systems: A market diffusion model considering individual consumer behaviour and preferences', *Appl. Energy*, vol. 205, pp. 1560–1570, Nov. 2017, doi: 10.1016/j.apenergy.2017.08.159.

[21] R. E. Bird and R. L. Hulstrom, 'Simplified clear sky model for direct and diffuse insolation on horizontal surfaces', Solar Energy Research Inst., Golden, CO (USA), SERI/TR-642-761, Feb. 1981. doi: 10.2172/6510849.